Molecular Mode of Action of a Covalently Inhibiting Peptidomimetic on the Human Calpain Protease Core[†,‡]

Qingshan Li,[§] Robert P. Hanzlik,[§] Robert F. Weaver,[||] and Ernst Schönbrunn*[,§]

Department of Medicinal Chemistry and Department of Molecular Biosciences, University of Kansas, Lawrence, Kansas 66045

Received October 12, 2005; Revised Manuscript Received November 28, 2005

ABSTRACT: Calpain is a nearly ubiquitous Ca^{2+}-activated proteolytic enzyme whose precise physiological function is unknown. However, aberrant Ca^{2+} homeostasis in the course of cellular injuries and certain diseases of the CNS appears to activate calpain, in turn promoting the degradation of key cytoskeletal and membrane proteins. Hyperactive calpain has also been implicated in various aging phenomena and diseases of late life. Therefore, calpain is considered a potential therapeutic target in preventing degenerations of many kinds. Despite its potential medicinal importance, known structural information about μ-calpain is limited to that from the rat enzyme. We have determined the crystal structure of the human μ-calpain protease core (hμI-II) containing a Gly213Ala mutation and covalently inactivated by a peptidomimetic ($ZLLYCH_2F$) at 2.0 Å resolution. The methylene carbon of the inhibitor is bound to Cys115. Additional hydrogen bonding and hydrophobic interactions between active site residues and the inhibitor, including an intermolecular antiparallel β-sheet arrangement characteristically observed with members of the papain family of cysteine proteinases, help to stabilize the complex and orient the inhibitor. The terminal ZL portion of the inhibitor is solvent-exposed and highly flexible, and is thus not involved in specific binding interactions with the enzyme. Two large enzyme regions flanking the active site are highly flexible; they may be important in recognition of calpain's natural *protein* substrates and in positioning them for catalysis. The implications for drug design are discussed.

Calpains make up a family of Ca^{2+}-dependent cytoplasmic cysteine proteinases found in mammals, insects, nematodes, and yeast (*1*−*3*). In mammals, at least 14 different calpain genes are known to be expressed in various tissues, but the m- and μ-isoforms are the most widely expressed (*1*, *4*, *5*). These isoforms, together with their endogenous inhibitor calpastatin (*6*), are believed to play key roles in Ca^{2+}-dependent regulation of physiological processes such as the cell cycle, cytoskeletal remodeling, apoptosis, and cellular motility via the limited proteolysis of selected target proteins, although their precise function is not fully understood (*7*−*10*). Activation of calpain, as well as mutations that alter calpain activity, has been implicated in several devastating human pathologies, including muscular dystrophy, cardiac and cerebral ischemia-reperfusion injury, Alzheimer's and other neurodegenerative diseases, rheumatoid arthritis, and cataract formation (*2*, *5*, *11*−*14*).

The m- and μ-calpains are both heterodimers consisting of a common regulatory 30 kDa subunit having a chaperone-like function, and one of two isoform-specific catalytic 80 kDa subunits. Both forms absolutely require Ca^{2+} for activity; however, the concentration of Ca^{2+} required to activate m-calpain is in the millimolar range, whereas μ-calpain is activated by 10−50 μM Ca^{2+} (*15*, *16*). Autolysis of m- and μ-calpain leads to the generation of protease core fragments or "mini-calpains" (ca. 39−40 kDa) derived from domains I and II of the large subunit and containing the catalytic triad residues Cys115, His272, and Asn296 (*17*, *18*). The rat mini-μ-calpain (μI-II) retains a modest degree of catalytic activity but lacks the calpastatin-binding sites present in calpain domains III, IV, and VI (*6*). Thus, once formed in vivo, it could have significant implications for cellular pathology, because it would not be subject to the regulation by calpastatin (*18*, *19*). In contrast, the catalytic activity of rat mini-m-calpain (mI-II) is barely detectable using small peptidic substrates. The enzymatic activity of rat μI-II appears to be modulated by two distinct Ca^{2+} sites (*20*, *21*). Its three-dimensional structure resembles closely that of papain, a plant cysteine protease that is Ca^{2+}-independent, and key catalytic residues are strictly conserved between calpain and papain (*19*). In addition to the Ca^{2+} dependence of the μI-II autolysis product, certain structural elements appear to impact its enzymatic activity. In particular, whereas rat μI-II has an alanine residue at position 203, the much less active rat mI-II has a glycine at this position. Mutating this glycine to alanine significantly enhances the activity of the mI-II protease core, presumably by stabilizing an α-helix in the protein (*18*). Interestingly, human μI-II also has a glycine at the equivalent position (Gly213). We therefore included in

[†] Financial support for this work was provided by the University of Kansas (RDF00190). Diffraction data were collected in the University of Kansas Protein Structure Lab, funded by a COBRE grant (5P20-RR017708) from the National Center for Research Resources of the National Institutes of Health.

[‡] The atomic coordinates and structure factors (entry 1ZCM) have been deposited in the Protein Data Bank.

* To whom correspondence should be addressed: Department of Medicinal Chemistry, University of Kansas, 4040a Malott Hall, Lawrence, KS 66045. Phone: (785) 864-4503. Fax: (785) 864-5326. E-mail: eschoenb@ku.edu.

[§] Department of Medicinal Chemistry.

[||] Department of Molecular Biosciences.

10.1021/bi052077b CCC: $33.50
Published on Web 12/24/2005

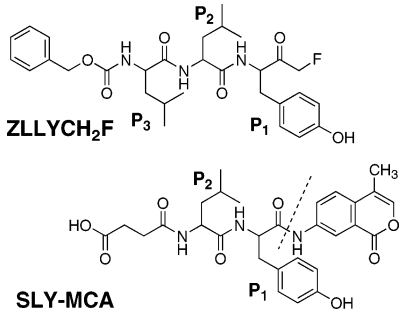

FIGURE 1: Structures of SLY-MCA and $ZLLYCH_2F$. Residue positions are designated P_1-P_3 in the direction from the scissile bond toward the N-terminus of the protein or peptide substrate according to the nomenclature of Schechter and Berger (*29*).

our studies both the Gly213Ala mutant of the hμI-II protease core as well as wild-type hμI-II.

Despite the medical importance of calpain, the available three-dimensional calpain structures are limited to those from the rat. Here we report that the in vitro activity of the human μ-calpain protease core (hμI-II) is greatly improved by mutation of Gly213 to Ala. The X-ray structure of this mutated protease core, covalently inactivated by the substrate analogue inhibitor $ZLLYCH_2F$, reveals the enzyme active site and its interactions with the inhibitor in atomic detail. The results should aid future structure-based design approaches to improved calpain inhibitors as potential therapeutic agents.

EXPERIMENTAL PROCEDURES

Materials. The peptidyl fluoromethyl ketone inhibitor Cbz-Leu-Leu-Tyr-CH_2F ($ZLLYCH_2F$) and the fluorogenic assay substrate succinyl-Leu-Tyr-7-amino-4-methylcoumarin (SLY-MCA) were obtained from Calbiochem (La Jolla, CA). Their structures are shown in Figure 1. 7-Amino-4-methylcoumarin and casein (No. C-5890) were obtained from Sigma-Aldrich (St. Louis, MO). Other reagents were purchased from standard commercial suppliers. Protein concentrations were determined using the Bradford assay based on Coomassie Blue stain (Pierce, Rockford, IL) with bovine serum albumin as the reference standard.

Preparation of the Mini-μ-calpain Autolysis Product hμI-II from Recombinant Human μ-Calpain (rhμ-Calpain) by Autolysis. rhμ-Calpain was expressed and purified according to the method of Meyer et al. (*22*) with slight modifications. In our study, Sf9 cells rather than Sf21 cells were used for calpain expression and the final purification step employed a Resource Q column (Amersham, Piscataway, NJ) rather than a Mimetic Red 2 column. The recombinant virus (AcNPV-hCANPI-2−5) containing the genes of the large and small subunits of rhμ-calpain was provided by S. Meyer (Cephalon, West Chester, PA). rhμI-II was produced by the autolysis reaction of rhμ-calpain in the presence of calcium as follows. The reaction mixture contained 0.5 mg/mL calpain, 0.5 mM free Ca^{2+}, and 10 mM β-mercaptoethanol in 50 mM Tris-HCl buffer (pH 7.3). After autolysis for 5 h at room temperature, the autolysis products were separated by anion exchange chromatography on a Resource Q column. The purified autolysis product was analyzed by SDS−PAGE, by activity assay using casein (see below) as well as SLY-MCA (*18*), by the calcium dependence of its inactivation by $ZLLYCH_2F$, and by MALDI-TOF mass spectrometry of the covalently inactivated product.

Cloning of hμI-II and Site-Directed Mutagenesis of Gly213 to Ala. The autolysis segment hμI-II extends from residue Gly29, which defines the start of domain I, to residue Tyr371. This region was amplified by PCR from the human μ-calpain large subunit using Pfu DNA polymerase (Stratagene, La Jolla, CA). The sense primer, 5′-CTGGCCATGGGCCGC-CATGAGAATGCC-3′, contains the Met initiation codon and an NcoI site, and the antisense primer, 5′-CCGCCGC-CACTCGAGTCAGTAGAGTGTGGTGTTCC-3′, contains a stop codon and an XhoI site. The amplified PCR fragment was purified with a Qiaquick PCR purification kit (Qiagen, Waltham, MA) and digested with restriction enzymes NcoI and XhoI. The restriction segment was further purified and ligated into the pET24d(+) vector (Novagen, Madison, WI) using T4 ligase (Promega, Madison, WI) according to the protocols provided by the manufacturers. The recombinant plasmid was transformed into BL21(DE3) *Escherichia coli* (Stratagene). Site-directed mutagenesis of Gly213 to Ala was completed by PCR with two primers containing this mutation (the sense primer, 5′-AGAGGCTTTTGAGGAC-3′, and the antisense primer, 5′-GTCCTCAAAAGCCTCT-3′). The sequences of hμI-II and the G213A mutant genes were confirmed by DNA sequencing.

Expression and Purification of hμI-II and the hμI-II Gly213Ala Mutant. The *E. coli* BL21(DE3) containing the recombinant plasmid was cultured in LB medium at 37 °C to an OD of 0.4−0.8 (600 nm) and then induced by 1 mM IPTG at 16 °C for 38 h. Wild-type hμI-II and the Gly213Ala mutant analogue were each purified using the same protocol on an ÅKTA FPLC system (Amersham). The buffer that was used consisted of 50 mM Tris-HCl (pH 7.4) containing 5 mM DTT and 1 mM EDTA. The protein was first eluted from a Q-Sepharose Fast Flow column by a 50 to 150 mM NaCl gradient, followed by elution with water from a HiLoad phenyl-Sepharose colum. It was further purified by a MonoQ column using a gradient of 50 to 150 mM NaCl. Finally, a HiLoad Superdex 200 column eluted with buffer yielded the pure protein.

Activity of hμ-Calpain, hμI-II, and Gly213Ala hμI-II toward Casein. The degradation of casein was analyzed by SDS−PAGE and HPLC. Commercial casein consists of two major and several minor isoforms as seen on HPLC. A single major isoform of casein was separated from the others by chromatography over a Resource Q column. Proteins were eluted by a gradient from 50 to 250 mM NaCl in 50 mM Tris-HCl (pH 7.4) and 1 mM EDTA. The major isoform of casein was further purified by gel filtration using a HiLoad Superdex 200 (16/60) column and eluted with 50 mM Tris-HCl (pH 7.4) and 1 mM EDTA. The molecular weight of the purified isoform was ca. 24 000 as estimated by SDS−PAGE. Enzyme activity assays were performed at 22−23 °C in a final volume of 0.5 mL of 50 mM Tris-HCl buffer (pH 7.3), 10 mM β-mercaptoethanol, 330 μM casein, and 6 mM $CaCl_2$ (2 mM $CaCl_2$ for μ-calpain) containing either 42 nM μ-calpain, 2.4 μM Gly213Ala hμI-II, or 28 μM hμI-II. Periodically, a 20 μL aliquot of the reaction mixture was combined with 5 μL of 100 mM EDTA (to stop the reaction) and analyzed by SDS−PAGE or HPLC. The latter was carried out using a VYDAC protein and peptide C-18 column (218TP54, 4.6 mm × 250 mm) eluted at a flow rate of 1

Table 1: Kinetic Constants for Hydrolysis of the Casein Isoform and SLY-MCA by hμ-Calpain, hμI-II, and Gly213Ala hμI-II

	hμI-II	Gly213Ala hμI-II	hμ-calpain	rat μI-II[a]
casein isoform				
turnover (s^{-1})	0.00109 ± 0.00015	0.135 ± 0.009	4.37 ± 0.35	
relative activity	1	125	2300	
SLY-MCA				
k_{cat} ($\times 10^{-6}$ s^{-1})	2.17 ± 0.19	1024 ± 57	24700 ± 1800	427 ± 47
K_m (mM)	1.36 ± 0.23	1.46 ± 0.17	1.05 ± 0.17	0.335 ± 0.006
k_{cat}/K_m (M^{-1} s^{-1})	0.0016 ± 0.0003	0.701 ± 0.090	23.5 ± 4.17	1.27 ± 0.142
relative k_{cat}/K_m	1	440	14700	

[a] Rat μI-II data from ref *19*.

mL/min with a gradient of solution B (10% H_2O, 90% CH_3CN, and 0.1%TFA) in solution A (80% H_2O, 20% CH_3CN, and 0.1% TFA) with solution B increasing from 0 to 30% over the course of 20 min and from 30 to 40% over the course of 8 min. The enzyme activity was estimated by assessing the disappearance of the substrate (purified casein isoform) on HPLC and by the generation of lower-molecular weight bands on SDS−PAGE. The retention time for the casein isoform was 26.8 min; significant product peaks appeared at retention times of 9.7, 10.8, 11.9, 15.9, 22.2, 22.8, 23.7, and 24.1 min.

Activity of hμ-Calpain, hμI-II, and Gly213Ala hμI-II toward the Synthetic Peptide Substrate SLY-MCA. Hydrolysis of SLY-MCA was monitored by fluorescence at 460 nm (excitation at 380 nm) at 22−23 °C according to the manufacturer's directions and ref *18*. The reaction mixture (0.5 mL total) contained 50 mM Tris-HCl (pH 7.5), 4% DMSO, 5 mM β-mercaptoethanol, 200 mM NaCl, 6 mM $CaCl_2$ (2 mM $CaCl_2$ for hμ-calpain), varying substrate concentrations, and either 91 nM calpain, 2.5 μM Gly213Ala hμI-II, or 15 μM wild-type hμI-II. The amount of product that formed was determined by comparison to solutions of authentic 7-amino-4-methylcoumarin.

Preparation of the Complex of the hμI-II Gly213Ala Mutant Covalently Bound with ZLLYCH$_2$F. The reaction mixture contained 1.0 mg/mL hμI-II Gly213Ala mutant, 10 mM β-mercaptoethanol, 15 mM $CaCl_2$, and 0.15 mM $ZLLYCH_2F$ in 0.1 M Tris-HCl buffer (pH 7.3). The reaction mixture was maintained at room temperature in the dark for 3 h, applied to a PD10 gel filtration column (Amersham), and eluted with freshly prepared 20 mM HEPES (pH 7.5) containing 10 mM DTT and 8 mM $CaCl_2$. For crystallization, the enzyme−inhibitor complex was first concentrated using a Centricon YM-30 membrane filtration device (Millipore). After a 2.0 mL aliquot of protein solution (ca. 1 mg/mL) was concentrated to ca. 0.5 mL, an additional 1.5 mL of protein solution was added, and the mixture was concentrated again to a final volume of 0.5 mL; at this point, ca. 30% of the protein was in solution and 70% had precipitated above the membrane. The supernatant was removed by pipet, and the pellet was dissolved in 0.3 mL of a solution containing 200 mM HEPES (pH 7.5), 10 mM DTT, 25 mM $CaCl_2$, and 1 M NaCl. This solution was further concentrated to 20−30 mg of protein/ml. After the fact that inactivation was complete had been verified (SLY-MCA assay), this solution was used for protein crystallization experiments as described below.

Crystallography. Crystallization of hμI-II Gly213Ala inactivated by $ZLLYCH_2F$ was performed by the hanging drop vapor diffusion method at 19 °C. Crystals were grown by the salting-in method, equilibrating 6 μL droplets of the concentrated enzyme−inhibitor complex (prepared as described above) against 0.5 mL of 6 mM DTT. Diffraction data were recorded at −180 °C using the rotation method on a single flash-frozen crystal [cryosolvent, glycerol; detector, R-axis IV^{++} image plate; X-rays, Cu Kα, focused by mirror optics; generator, Rigaku RU300 (MSC, The Woodlands, TX)]. The data were reduced with XDS (*23*); CNS (*24*) was employed for phasing and refinement, and model building was performed with O (*25*). The structures were determined by molecular replacement using the μ-calpain protease core from rat (PDB entry 1KXR) (*19*), stripped of solvent molecules, as a search model. Refinement was performed using data to the highest resolution with no σ cutoff applied. Six rounds of minimization, simulated annealing (starting temperature of 2500 K) and restrained individual *B*-factor refinement were carried out. Data collection and refinement statistics are summarized in Table 2. Figures 4−6 were drawn with Molscript (*26*) and Raster3D (*27*); Figure 4 (middle) was drawn with Bobscript (*28*) and Raster3D.

Table 2: Summary of Data Collection and Structure Refinement[a]

space group	$P2_12_12_1$
unit cell dimensions	$a = 50.4$ Å, $b = 62.7$ Å, $c = 99.3$ Å, $\alpha = \beta = \gamma = 90°$
no. of molecules/asymmetric unit	1
no. of protein atoms	2605 (average B value = 24.8 Å^2)
no. of alternate atom positions	34
no. of ligand atoms	39 (average B value = 37.4 Å^2)
no. of solvent molecules	206 (average B value = 32.0 Å^2)
no. of Ca^{2+} ions	2 (average B value = 17.4 Å^2)
rmsd[b] for bond lengths (Å)	0.007
rmsd[b] for bond angles (deg)	1.4
resolution range	20.0−2.0 Å (2.1−2.0 Å)
no. of measured reflections	152535 (19518)
no. of unique reflections	21280 (2800)
completeness (%)	97 (94.8)
$I/\sigma I$	26.6 (9.9)
R_{mrgd-F}[c] (%)	3.6 (10.3)
R_{meas}[c] (%)	4.8 (20.6)
R_{cryst}[d] (%)	18.2
R_{free}[e] (%)	22.3

[a] Values in parentheses refer to the highest-resolution shell. [b] Root-mean-square deviation from ideal values. [c] R_{meas} and R_{mrgd-F} as defined by Diederichs and Karplus (*36*) are quality measures of the individual intensity observations and the reduced structure factor amplitudes, respectively. [d] $R_{cryst} = 100\sum|F_{obs} - F_{model}|/\sum F_{obs}$, where F_{obs} and F_{model} are observed and calculated structure factor amplitudes, respectively. [e] R_{free} is the R_{cryst} calculated for 1064 randomly chosen unique reflections, which were excluded from the refinement.

RESULTS AND DISCUSSION

The m-calpain protease core from rat (mI-II) displays negligible activity against SLY-MCA, a commonly used

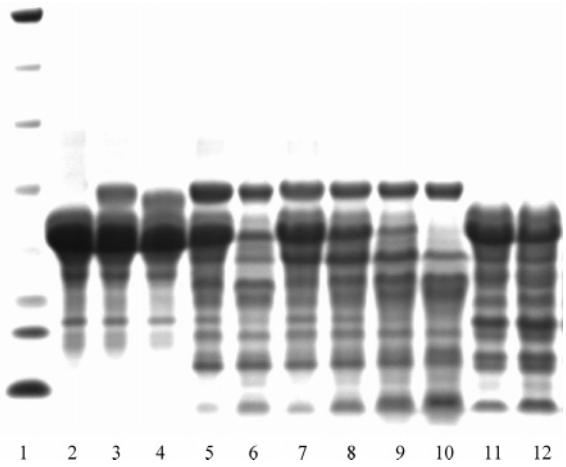

FIGURE 2: SDS−PAGE analysis of digestion of casein by hμI-II, hμI-II G213A, and rhμ-calpain: lane 1, molecular mass standards (193, 103, 60, 41, 17, 14, and 6 kDa, respectively, from top to bottom); lane 2, casein substrate; lane 3, mixture of casein and Gly213Ala hμI-II (15:1 ratio); lane 4, mixture of casein and Gly213Ala hμI-II previously inactivated by ZLLYCH$_2$F (15:1 ratio) with 6 mM $CaCl_2$ after incubation for 3 h; lanes 5 and 6, mixture of casein and hμI-II (10:1 ratio) with 10 mM $CaCl_2$ incubated for 1 and 3 h, respectively; lanes 7−10, mixture of casein with Gly213Ala hμI-II (25:1 ratio) and 10 mM $CaCl_2$ incubated for 3, 6, 9, and 18 min, respectively; and lanes 11 and 12, mixture of casein and rhμI-II (3000:1 ratio) with 10 mM $CaCl_2$ incubated for 3 and 6 min, respectively.

fluorogenic substrate of calpain. Apparently, this is a result of the truncation of the full-length enzyme. However, the activity of mI-II is significantly increased after Gly203 is mutated to Ala. This mutation appears to stabilize an α-helix, thereby preventing the Trp106 side chain from protruding into the active site cleft (*18*). The corresponding residue in human μ-calpain is Gly213; we therefore made the Gly213Ala mutant of hμI-II and included it in our studies.

Activity Measurements. Casein was used as a protein substrate to compare the activities of full-length recombinant human μ-calpain, the μI-II autolysis fragment, and the Gly213Ala mutant of the latter. The turnover numbers for these species were 4.37, 0.135, and 0.00109 s^{-1}, respectively (Table 1). Since these values were calculated from the reduction of the casein peak as detected by HPLC, and did not take into account the further digestion of the initial casein fragments, the actual turnover numbers of these enzymes may be several times higher than the numbers reported here. As is evident from SDS−PAGE, several casein degradation products are formed (Figure 2). Although the relative activities of hμI-II, the Gly213Ala mutant of hμI-II, and whole hμ-calpain toward the purified casein isoform vary in the ratio of ca. 1:125:2300, both the proteolysis products formed and their respective product ratios appear to be very nearly identical (Figure 2). As in the data obtained for casein, wild-type μI-II hydrolyzes SLY-MCA at an extremely slow rate ($k_{cat} = 2.17 \times 10^{-6}$ s^{-1}; Figure 3 and Table 1). As seen in Table 1, introducing the Gly213Ala mutation increases k_{cat} substantially (ca. 470-fold), bringing it close to the value for rat μI-II (which intrinsically contains Ala at this position, Ala203) but still leaving it far short of k_{cat} for the intact hμ-calpain. Since the K_m values for SLY-MCA were very similar for all three human enzyme forms, the ca. 15000-fold variation in their catalytic efficiencies (k_{cat}/K_m) is determined largely by changes in k_{cat}. Thus, full-length μ-calpain and

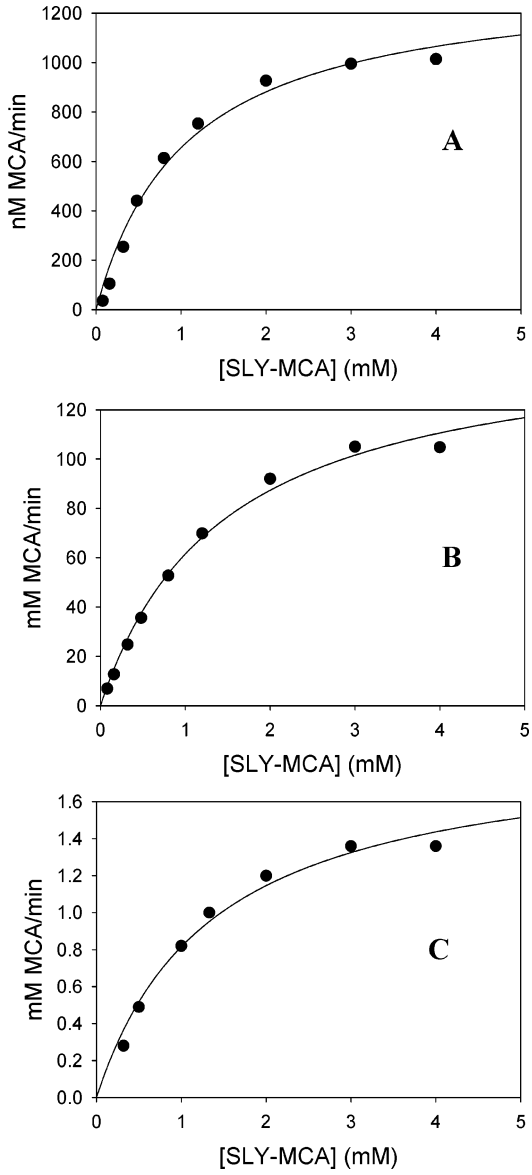

FIGURE 3: Kinetics of SLY-MCA hydrolysis. Hydrolysis rates of SLY-MCA were determined for 91 nM μ-calpain (A), 2.5 μM Gly213Ala hμI-II (B), and 15 μM hμI-II (C). Data were fit to the Michaelis−Menten equation. The derived kinetic constants are included in Table 1.

its wild-type and mutant protease cores differ only in their relative catalytic efficiencies; their substrate selectivity with respect to SLY-AMC and casein cleavage products that formed appears to be unaltered. Because replacing Gly213 with Ala resulted in a greatly enhanced activity of the hμI-II protease core, covalent inactivation with the substrate analogue ZLLYCH$_2$F and structure elucidation were performed with Gly213Ala mutant hμI-II.

Crystal Structure of the Inactivated Protease Core. Gly213Ala μ-I-II was inactivated with ZLLYCH$_2$F in the presence of Ca^{2+} and subsequently crystallized. Structure determination at 2.0 Å resolution revealed the inhibitor covalently bound to Cys115 (Table 2 and Figure 4). The final model contains residues 33−353, two Ca^{2+} ions, the covalently bound inhibitor, and 206 solvent molecules. N-Terminal residues 29−32 and C-terminal residues 354−371 are disordered and were not included in the refinement. The inhibitor was modeled into the electron density map according to the clear density of its covalent bond with

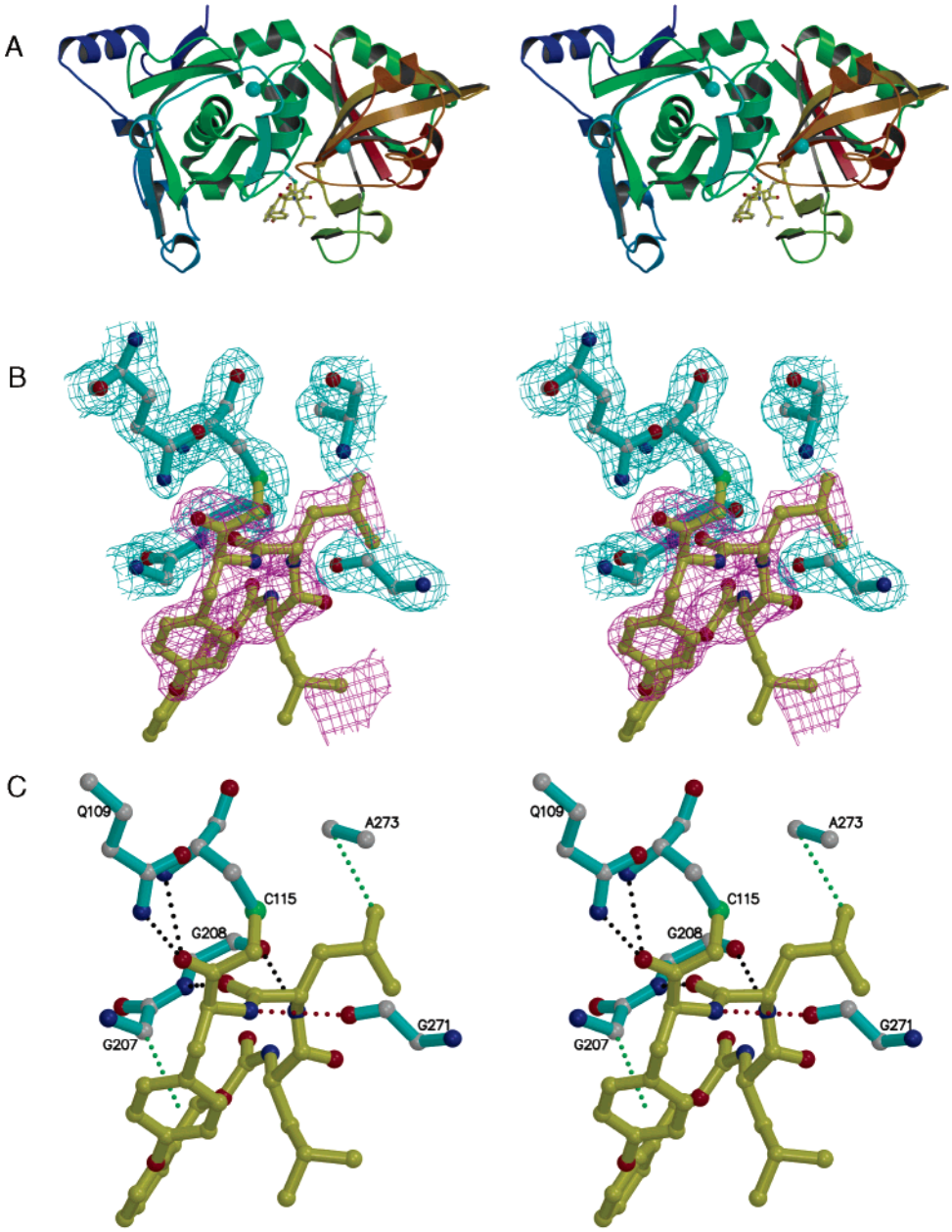

FIGURE 4: Covalent modification of human calpain by ZLLYCH$_2$F. (A) Overall fold of the human calpain dead-end complex color-traced from N-terminal residue Asn33 (blue) to C-terminal residue Leu353 (red). The inhibitor is drawn in ball-and-stick format (yellow). Turquoise balls represent the two Ca^{2+} ions. (B) Electron densities derived from a $2F_o - F_c$ Fourier synthesis (cyan) and a $F_o - F_c$ synthesis (red) to 2.0 Å resolution, omitting the model of the inhibitor during the refinement (one cycle of simulated annealing and *B*-factor refinement). The $2F_o - F_c$ map was contoured at 1σ and the $F_o - F_c$ map at 3σ. The overlaid structure model is color-coded according to atom type: carbon atoms of the inhibitor colored yellow, carbon atoms of the enzyme gray, nitrogen atoms blue, oxygen atoms red, and sulfur atoms green. Density is missing for the ZL part of the inhibitor. (C) Binding pattern of the peptidomimetic around Cys115. Hydrogen bonding interactions are represented by black dotted lines and hydrophobic forces by green dotted lines. The red dotted line represents a hydrogen bond typically observed between peptidomimetics and papain or rat calpain; the distance of 3.5 Å observed here indicates a weak hydrogen bonding interaction. The coordinate error is 0.19 Å (estimated from the Luzzati plot) and 0.09 Å (estimated from Sigmaa).

Cys115 and the adjacent P_1-Tyr and P_2-Leu moieties [nomenclature of Schechter and Berger (*29*)]. The N-terminal benzyl moiety and the P_3-Leu moiety of the inhibitor are disordered (Figure 4) but were included throughout the refinement.

The inhibitor is largely solvent-exposed, located in a cleft between the N-terminal domain (residues 33−219) and the C-terminal domain (residues 220−353) of the protease core (Figure 5). Although the covalent linkage with Cys115 anchors the inhibitor to the active site, the residues of the catalytic triad, His272 and Asn296, do not interact with the inhibitor. Instead, hydrogen bonding and hydrophobic interactions between the enzyme and the P_1-Tyr and P_2-Leu residues of the inhibitor also appear to stabilize the conformation of the inhibitor. The P_1CO group of the inhibitor hydrogen bonds to the side chain amide of Gln109 and to the backbone NH group of Cys115 (bond lengths of 3.02 and 3.21 Å, respectively); these interactions comprise the "oxyanion hole" that is characteristic of the cysteine (and serine) proteinases. Three other hydrogen bonds, including P_1NH−OC(Gly271) (3.51 Å), P_2CO−NH(Gly208) (2.94 Å), and P_2NH−OC(Gly208) (3.02 Å) bonds, form an antiparallel

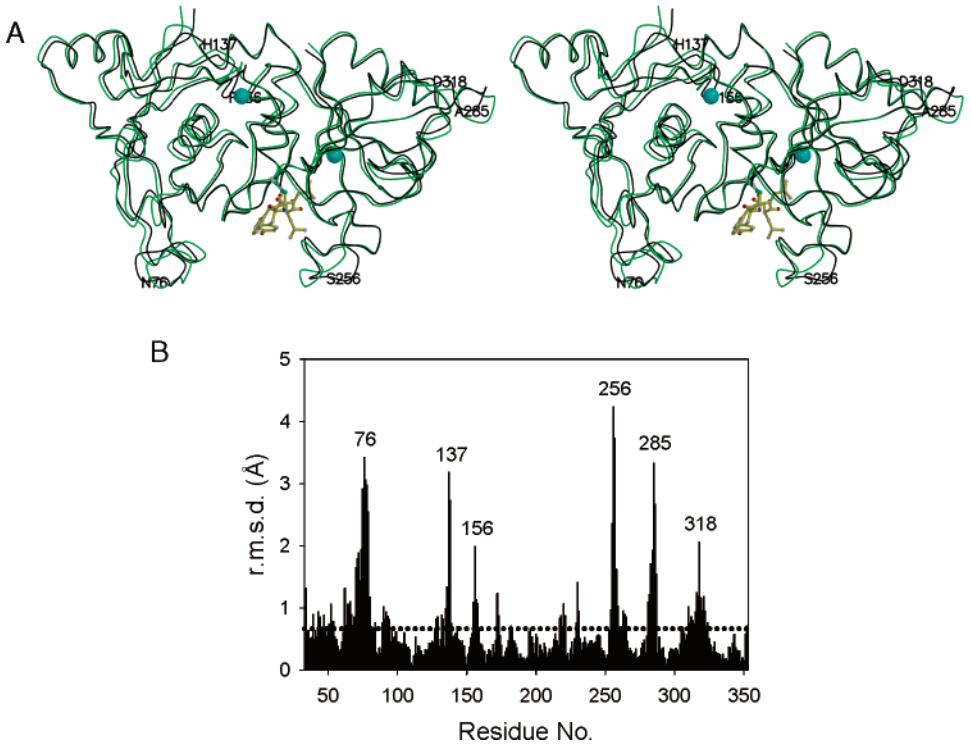

FIGURE 5: Comparison of the human and rat calpain structures. (A) Stereopair of the superimposed backbone structures of the human (black, this work) and rat (green, PDB entry 1Tl9) calpain. Rat calpain was overlayed with Lsqkab (*37*) using the main chain atoms of residues 33−353. (B) Root-mean-square deviation (rmsd) of the main chain atoms of human and rat calpain. The average rmsd value is 0.67 Å (···). The peaks above 2 Å rmsd are labeled with the corresponding residues; their location in the overall structure is indicated in panel A.

β-sheet structure in which the inhibitor spans the gap between the two walls of the active site cleft in a fashion that again is characteristic of cysteine proteinases in the papain family. For papain itself, the hydrogen bonds of the oxyanion hole stabilize the tetrahedral intermediate formed by peptide aldehyde inhibitors by up to 2−3 kcal/mol, suggesting that they also contribute directly to catalysis via transition state stabilization (*30*). Likewise, the P_2NH hydrogen bond in papain contributes up to 2.8 kcal/mol to the stabilization of transition states of substrates and the binding of transition state analogue inhibitors (*31*, *32*). Although the putative P_1-NH−OC(Gly271) hydrogen bond in the calpain structure appears to be unusually long, it is reported to be even longer (3.8 Å) in the case of papain alkylated by the substrate analogue Z-Phe-Ala-CH_2Cl (*33*). Despite its great length in the papain example, this feature still contributes up to 1.2 kcal/mol to the stabilization of transition states of substrates and the binding of transition state analogue inhibitors (*31*, *32*). In the case presented here, the potential weakness of this bond (implied by its length) may be offset by a close (3.6 Å) interaction of the aromatic π-system of the P_1-Tyr residue with the methylene of Gly207; the only other hydrophobic contact is between the methyl group of Ala273 and the side chain of the inhibitor P_2-Leu (see Figure 4). In papain, these five hydrogen bonds not only contribute individually but also interact cooperatively in catalysis and inhibitor binding, a factor that may be important to consider in terms of inhibitor design (see below).

During the course of this work, two structures of the rat calpain protease core inactivated by the inhibitors leupeptin and E64 were published (*11*). Comparison of the rat enzyme inactivated by the peptide aldehyde leupeptin (Ac-Leu-Leu-Arg-H) and the human enzyme inactivated by ZLLYCH_2F reveal the same principal set of noncovalent interactions of these two peptidomimetics within the active site. The overall structures of the human and rat calpain protease cores are almost identical (Figure 6): the root-mean-square deviation (rmsd) is 0.66 Å between 321 equivalent pairs of Cα atoms. The largest differences occur in the backbone around residues His137 and Phe156 of the N-terminal domain and residues Val257 and Gly286 of the C-terminal domain. These regions are solvent-exposed and quite flexible, particularly around positions 257 and 286 (see below). As expected, the two Ca^{2+} ions bind to human calpain through the same coordination pattern that is found in the rat enzyme. Apparently, inactivation by the peptidomimetic does not perturb the overall structure or the active site of the enzyme.

The relatively compact structure of the calpain protease core, which gives rise to the high diffraction quality of the crystals, also displays a surprisingly high degree of flexibility in larger areas at the surface of the molecule, which is reflected in the relatively high crystallographic R_{free} value of 22% (Table 2). It is likely that some of these regions contribute to heteromeric protein−protein interactions between the enzyme and its protein substrates. In particular, the large loop structures flanking the active site may be crucial for substrate recognition, placing the protein to be cleaved over the active site groove (Figure 6). This conclusion was also reached for the rat enzyme (*11*).

Implications for Drug Design. Although calpain is a prime target for the design of future drugs, little is known at the atomic level about the action of small molecule inhibitors on this medicinally important enzyme. The presented structure of hμI-II inactivated by ZLLYCH_2F provides evidence

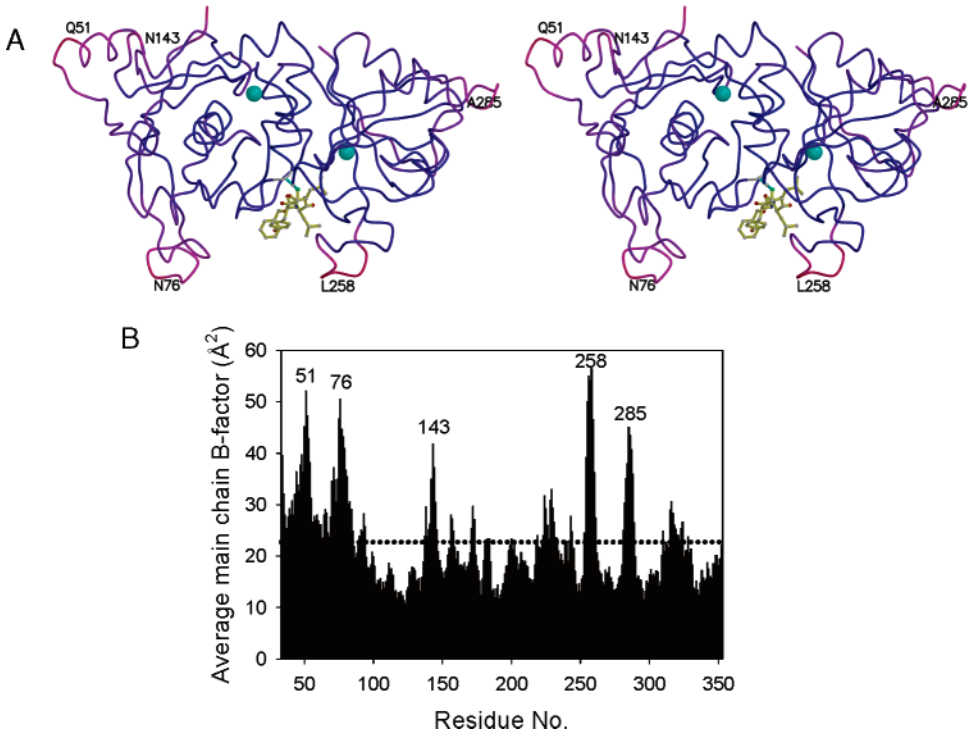

FIGURE 6: Flexible regions within the human calpain protease core. (A) Stereopair of the backbone of human calpain color-traced according to temperature factors from blue (10 Å^2) to red (70 Å^2). The regions around Asn76 and Val257 may constitute parts of the binding sites for calpain's natural substrates. (B) Main chain *B*-factor distribution of human calpain. The average *B*-factor of all main chain atoms is 22.7 Å^2 (···). The peaks above 40 Å^2 are labeled with the corresponding residues; their location in the overall structure is indicated in panel A.

that even covalent modification of the active site Cys residue does not result in major conformational changes in calpain's protease core. This makes calpain a superb target for the computational design of novel active site-directed inhibitors. The structure also suggests that, for peptidomimetics such as ZLLYCH$_2$F, only the residues adjacent to the electrophilic fluorine interact with enzyme residues. Therefore, variations in the "N-terminal" region of such peptide analogues may be helpful in increasing the number of noncovalent interactions to achieve tighter and more selective binding. However, the covalent modification of an enzyme residue, such as Cys115 in human calpain, by a small molecule is rarely target specific and is thus often considered to be unsafe pharmaceutically. The potent calpain inactivator ZLLYCH$_2$F, for example, is sufficiently reactive toward organic mercapto that a 15 min preincubation of ZLLYCH$_2$F in buffer containing mercaptoethanol, prior to combining it with calpain and calcium, results in the complete loss of its inhibitory activity (unpublished observations).

The inactivated hμI-II structure presented here may offer a glimpse at the active site after the nucleophilic attack of Cys115 on one of its in vivo substrates has taken place. However, for drug design purposes, the structure of additional complexes between calpain and noncovalent inhibitors would be highly desirable for the identification of the high- and low-energy interactions that govern substrate recognition and transition state binding. Given that the catalytic site of calpain is solvent exposed, the remarkable selectivity of calpain for specific cleavages of specific natural substrates probably originates from the net energetics of a multitude of enzyme−substrate interactions. These would include the covalent interaction of the Cys115 thiolate with the scissile amide bond, several noncovalent interactions in the immediate vicinity of the catalytic site (both hydrogen bonding and hydrophobic), and more distal protein−protein interactions involving the two large flexible regions of the enzyme flanking the catalytic site (Figure 6). The latter presumed substrate recognition sites are more than ca. 16 Å from the catalytic site, too far to be reached by small molecules that are also anchored to or near Cys115. Thus, the design of potent inhibitors specific for calpain may require the use of larger bifunctional ligands that span the distance between the catalytic site and the putative distal substrate recognition sites. Alternatively, another approach could be to identify allosteric or other binding sites, which, when ligated by a small molecule, would render the enzyme unable to achieve its catalytically active conformation. Examples of this include the mercaptoacrylic acid derivative PD150606, which binds at a noncatalytic site in domain VI (*14*), and a 27-amino acid peptide which mimics the natural inhibitor calpastatin (*34*, *35*). In conclusion, more experimental data on various calpain−ligand complexes, and especially on calpain−protein complexes, are needed to more effectively apply structure-based drug design principles to this enzyme in the future.

ACKNOWLEDGMENT

We thank Dr. Sheryl Meyer and Cephalon, Inc., for providing the baculorivus AcNPV-hCANPI-2-5 used in this work.

REFERENCES

1. Farkas, A., Tompa, P., and Friedrich, P. (2003) Revisiting ubiquity and tissue specificity of human calpains, *Biol. Chem. 384*, 945−949.
2. Goll, D. E., Thompson, V. F., Li, H., Wei, W., and Cong, J. (2003) The calpain system, *Physiol. Rev. 83*, 731−801.
3. Perrin, B. J., and Huttenlocher, A. (2002) Calpain, *Int. J. Biochem. Cell Biol. 34*, 722−725.

4. Diaz, B. G., Moldoveanu, T., Kuiper, M. J., Campbell, R. L., and Davies, P. L. (2004) Insertion sequence 1 of muscle-specific calpain, p94, acts as an internal propeptide, *J. Biol. Chem. 279*, 27656−27666.
5. Chatterjee, P. K., Todorovic, Z., Sivarajah, A., Mota-Filipe, H., Brown, P. A., Stewart, K. N., Mazzon, E., Cuzzocrea, S., and Thiemermann, C. (2005) Inhibitors of calpain activation (PD150606 and E-64) and renal ischemia-reperfusion injury, *Biochem. Pharmacol. 69*, 1121−1131.
6. Wendt, A., Thompson, V. F., and Goll, D. E. (2004) Interaction of calpastatin with calpain: A review, *Biol. Chem. 385*, 465−472.
7. Janossy, J., Ubezio, P., Apati, A., Magocsi, M., Tompa, P., and Friedrich, P. (2004) Calpain as a multi-site regulator of cell cycle, *Biochem. Pharmacol. 67*, 1513−1521.
8. Glading, A., Lauffenburger, D. A., and Wells, A. (2002) Cutting to the chase: Calpain proteases in cell motility, *Trends Cell Biol. 12*, 46−54.
9. Tompa, P., Buzder-Lantos, P., Tantos, A., Farkas, A., Szilagyi, A., Banoczi, Z., Hudecz, F., and Friedrich, P. (2004) On the sequential determinants of calpain cleavage, *J. Biol. Chem. 279*, 20775−20785.
10. Liu, X., Van Vleet, T., and Schnellmann, R. G. (2004) The role of calpain in oncotic cell death, *Annu. Rev. Pharmacol. Toxicol. 44*, 349−370.
11. Moldoveanu, T., Campbell, R. L., Cuerrier, D., and Davies, P. L. (2004) Crystal structures of calpain-E64 and -leupeptin inhibitor complexes reveal mobile loops gating the active site, *J. Mol. Biol. 343*, 1313−1326.
12. Nixon, R. A. (2003) The calpains in aging and aging-related diseases, *Aging Res. Rev. 2*, 407−418.
13. Huang, Y., and Wang, K. K. (2001) The calpain family and human disease, *Trends Mol. Med. 7*, 355−362.
14. Lin, G., Chatopadhyay, D., Maki, M., Wang, K. K. W., Carson, M., Jin, L., Takano, E., Hatanaka, M., DeLucas, L. J., and Narayana, S. V. L. (1997) Crystal Structure of Calcium Bound Domain VI of Calpain at 1.9 Å Resolution and Its Role in Enzyme Assembly, Regulation, and Inhibitor Binding, *Nat. Struct. Biol. 4*, 529−547.
15. Hosfield, C. M., Elce, J. S., and Jia, Z. (2004) Activation of calpain by Ca^{2+}: Roles of the large subunit N-terminal and domain III-IV linker peptides, *J. Mol. Biol. 343*, 1049−1053.
16. Dutt, P., Spriggs, C. N., Davies, P. L., Jia, Z., and Elce, J. S. (2002) Origins of the difference in Ca^{2+} requirement for activation of mu- and m-calpain, *Biochem. J. 367*, 263−269.
17. Gabrijelcic-Geiger, D., Mentele, R., Meisel, B., Hinz, H., Assfalg-Machleidt, I., Machleidt, W., Moller, A., and Auerswald, E. A. (2001) Human micro-calpain: Simple isolation from erythrocytes and characterization of autolysis fragments, *Biol. Chem. 382*, 1733−1737.
18. Moldoveanu, T., Hosfield, C. M., Lim, D., Jia, Z., and Davies, P. L. (2003) Calpain silencing by a reversible intrinsic mechanism, *Nat. Struct. Biol. 10*, 371−378.
19. Moldoveanu, T., Hosfield, C. M., Lim, D., Elce, J. S., Jia, Z., and Davies, P. L. (2002) A Ca^{2+} switch aligns the active site of calpain, *Cell 108*, 649−660.
20. Moldoveanu, T., Jia, Z., and Davies, P. L. (2004) Calpain activation by cooperative Ca^{2+} binding at two non-EF-hand sites, *J. Biol. Chem. 279*, 6106−6114.
21. Pal, G. P., De Veyra, T., Elce, J. S., and Jia, Z. (2003) Crystal structure of a micro-like calpain reveals a partially activated conformation with low Ca^{2+} requirement, *Structure 11*, 1521−1526.
22. Meyer, S. L., Bozyczko-Coyne, D., Mallya, S. K., Spais, C. M., Bihovsky, R., Kawooya, J. K., Lang, D. M., Scott, R. W., and Siman, R. (1996) Biologically Active Monomeric and Heterodimeric Recombinant Human Calpain I Produced Using the Baculovirus Expression System, *Biochem. J. 314*, 511−519.
23. Kabsch, W. (1993) Automatic procession of rotation diffraction data from crystals of initially unknown symmetry and cell constraints, *J. Appl. Crystallogr. 26*, 795−800.
24. Brunger, A. T., Adams, P. D., Clore, G. M., DeLano, W. L., Gros, P., Grosse-Kunstleve, R. W., Jiang, J. S., Kuszewski, J., Nilges, M., Pannu, N. S., Read, R. J., Rice, L. M., Simonson, T., and Warren, G. L. (1998) Crystallography & NMR system: A new software suite for macromolecular structure determination, *Acta Crystallogr. B54*, 905−921.
25. Jones, T. A., Zou, J. Y., Cowan, S. W., and Kjeldgaard, M. (1991) Improved methods for building protein models in electron density maps and the location of errors in these models, *Acta Crystallogr. B47*, 110−119.
26. Kraulis, P. J. (1991) MOLSCRIPT: A program to produce both detailed and schematic plots of protein structures, *J. Appl. Crystallogr. 24*, 946−950.
27. Merrit, E. A., and Bacon, D. J. (1997) Raster3D: Photorealistic Molecular Graphics, *Methods Enzymol. 277*, 505−524.
28. Esnouf, R. M. (1997) An extensively modified version of MolScript that includes greatly enhanced coloring capabilities, *J. Mol. Graphics Modell. 15*, 132−134.
29. Schechter, I., and Berger, A. (1967) On the Size of the Active Site in Proteases. Papain, *Biochem. Biophys. Res. Commun. 27*, 157−162.
30. Menard, R., Plouffe, C., Laflamme, P., Vernet, T., Tessier, D. C., Thomas, D. Y., and Storer, A. C. (1995) Modification of the electrostatic environment is tolerated in the oxyanion hole of the cysteine protease papain, *Biochemistry 34*, 464−471.
31. Liu, S., and Hanzlik, R. P. (1993) The Contribution of Intermolecular Hydrogen Bonding to the Kinetic Specificity of Papain, *Biochim. Biophys. Acta 1158*, 264−272.
32. Berti, P. J., Faerman, C. H., and Storer, A. C. (1991) Cooperativity of Papain-Substrate Interaction Energies in the S2 to S2′ Subsites, *Biochemistry 30*, 1394−1402.
33. Drenth, J., Kalk, K. H., and Swen, H. M. (1976) Binding of Chloromethyl Ketone Substrate Analogues to Crystalline Papain, *Biochemistry 15*, 3731−3738.
34. Todd, B., Moore, D., Deivanayagam, C. C., Lin, G. D., Chattopadhyay, D., Maki, M., Wang, K. K., and Narayana, S. V. (2003) A structural model for the inhibition of calpain by calpastatin: Crystal structures of the native domain VI of calpain and its complexes with calpastatin peptide and a small molecule inhibitor, *J. Mol. Biol. 328*, 131−146.
35. Gil-Parrado, S., Assfalg-Machleidt, I., Fiorino, F., Deluca, D., Pfeiler, D., Schaschke, N., Moroder, L., and Machleidt, W. (2003) Calpastatin exon 1B-derived peptide, a selective inhibitor of calpain: Enhancing cell permeability by conjugation with penetratin, *Biol. Chem. 384*, 395−402.
36. Diederichs, K., and Karplus, P. A. (1997) Improved R-factors for diffraction data analysis in macromolecular crystallography, *Nat. Struct. Biol. 4*, 269−275.
37. Kabsch, W. (1976) A solution for the best rotation to relate two sets of vectors, *Acta Crystallogr. A32*, 922−923.

BI052077B